Available online at www.CivileJournal.org

Civil Engineering Journal

(E-ISSN: 2476-3055; ISSN: 2676-6957)

Vol. 11, No. 12, December, 2025

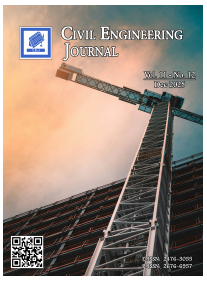

# Statistical (SPSS) Models: Ultimate Uplift Capacity of Horizontal Square Anchor Plate

Ali R. Daibil [1*], A'amal A. H. Al-Saidi [1]

[1] *Department of Civil Engineering, College of Engineering, University of Baghdad, Baghdad, Iraq.*

Received 29 July 2025; Revised 27 October 2025; Accepted 05 November 2025; Published 01 December 2025

**Abstract**

This paper examines the relationship between ultimate capacity and vertical displacement for single anchors and line anchor groups (1×2), (1×3), (1×4), and (1×5), in relation to the number of anchors and the embedment depth. Studies addressing statistical analysis in this area are limited; therefore, it was considered appropriate to conduct a statistical investigation to support this field with analytical results and to provide a foundation for future research. The statistical analysis for the single anchor plate indicated that the correlation between ultimate capacity, number of anchors, and embedment depth was strong, with acceptable values of R and $R^2$ and a well-fitting mathematical model. In contrast, vertical displacement showed insufficient mathematical representation when analyzed against the number of anchors and embedment depth, as vertical displacement is influenced by additional factors such as loading duration (creep effects), soil unit weight, plate shape and dimensions, internal friction angle, and moisture content, rather than by ultimate capacity alone. When the number of anchor plates in a group exceeds three, the vertical displacement at system failure increases due to the reduced strength of the soil associated with larger anchor groups.

*Keywords:* Mathematical Analysis; Group Anchor; Uplift Failure; Single Anchor Plate.

## 1. Introduction

In geotechnical engineering, anchor plates are widely used to stabilize walls, moor floating offshore structures, and serve similar purposes [1]. Owing to their high load-bearing capacity, weight, and ability to be installed at targeted locations, anchor plates are particularly effective in such applications [2]. Anchors are also beneficial in the construction of structures such as bridges and tunnels, where they provide structural support and help prevent sudden or rapid failure [3,4]. In the development of lightweight structures, such as towers and marine structures, the design, construction, and analysis of specialized tension soil-anchor systems are critical. When the tensile capacity of the soil-anchor system is sufficiently high to resist applied loads, the soil and anchor act as a unified system; however, when the tensile capacity is low, the soil–anchor system loses its integrity [5–8].

The tensile capacity of a soil-anchor system is mainly derived from the passive resistance of the soil located in front of the anchor plate [9]. Based on load transfer mechanisms, anchors are generally classified into two types: friction anchors and plate anchors. Friction anchors resist loads through frictional interaction between the soil and the anchor, whereas anchor plates resist uplift forces primarily through the bearing capacity of the soil beneath the anchor. Consequently, numerous experimental studies have investigated slope stability where friction anchors are installed [10–13].

* Corresponding author: ali.muhammad2201d@coeng.uobaghdad.edu.iq

http://dx.doi.org/10.28991/CEJ-2025-011-12-010

Wind loads can generate lateral reactions that exceed the self-weight of structures, and anchor plates are effective in resisting structural overturning due to lateral and uplift loads [14–18]. Previous studies indicate that anchor plates are widely used in geotechnical engineering to withstand lateral and uplift loads, particularly in lightweight structures that have limited resistance capacity. The bearing capacity of anchor plates depends on their weight and on the interaction between the anchor and the surrounding soil. Numerical studies have shown that embedment ratio and soil unit weight have a significant influence on the uplift capacity of anchor plates [19]. Results from PLAXIS 3D modeling indicate that anchor shape affects anchor resistance [20]; however, vertical displacement has not been sufficiently investigated through empirical equations. In large-diameter multi-plate soil anchors, if the number of plates is too small or the spacing between plates is excessively large, the system cannot fully utilize its ultimate uplift capacity [21]. Furthermore, existing research lacks comparative analysis between mathematical models to determine an optimal predictive model.

The ultimate capacity of an anchor plate can be enhanced through the use of reinforcement materials. For example, [22] employed geotextile reinforcement (referred to as grid-geotextile) with an opening size of 20 mm × 20 mm and reported an improvement in capacity ranging from 1.15 to 1.25 times compared with other geotextile opening sizes of 10 mm × 10 mm, 20 mm × 20 mm, and 30 mm × 30 mm. The purpose of the present study is to determine and analyze the ultimate bearing capacity of anchor plates, as well as the corresponding vertical displacement, with particular attention to variations in embedment depth. Mathematical models were derived and statistically compared, and optimal models were selected to describe the relationships among these variables for both single anchor plates and anchor plate groups.

## 2. Physical Model and Experimental Work

In this experimental study, a steel container with dimensions of 850 × 850 × 850 cm³ was used. The scale effect of the physical model was based on friction theory [23], and one face of the container was made of glass to allow observation of failure modes during anchor loading, as shown in Figure 1. The scale effect of the physical model was also considered based on the modified soil cone theory [19]. Square-shaped anchor plates with dimensions of 3 × 3 cm (B) were used, while the embedment depth (H) was varied. Line anchor groups consisting of (1×2), (1×3), (1×4), and (1×5) plates were welded together using a horizontal steel bar. Each group was arranged with a center-to-center spacing of S = 4D and was assumed to act as a large anchor (single anchor) [24].

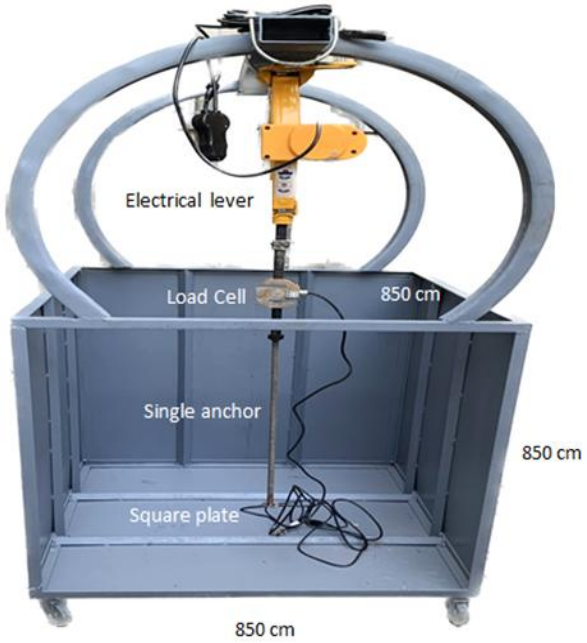


**Figure 1. Physical Model Test**

It is worth noting that the sandy soil used in this study was collected from the Najaf Sea area, and the in situ moisture content of 4% was adopted for the experiments. After installing the setup and filling it with sandy soil at a relative density (Dr) of 35%, the soil in the physical model was prepared using the raining method to achieve a loose sand state. The sand was deposited to a calculated height corresponding to a loose unit weight, resulting in a relative density of 35%. Different embedment depths (H = 2B, 3B, 4B, 5B, 6B, 7B, and 8B) were applied for both single anchor plates and line anchor plate groups. The system was then loaded until the ultimate uplift condition was reached. The average vertical displacement and ultimate uplift load were recorded using a load cell and two electronic linear variable differential transformers (LVDTs). Each test was repeated at least three times, and the results were considered acceptable when the difference between readings was less than 5%, as illustrated in Figure 2.

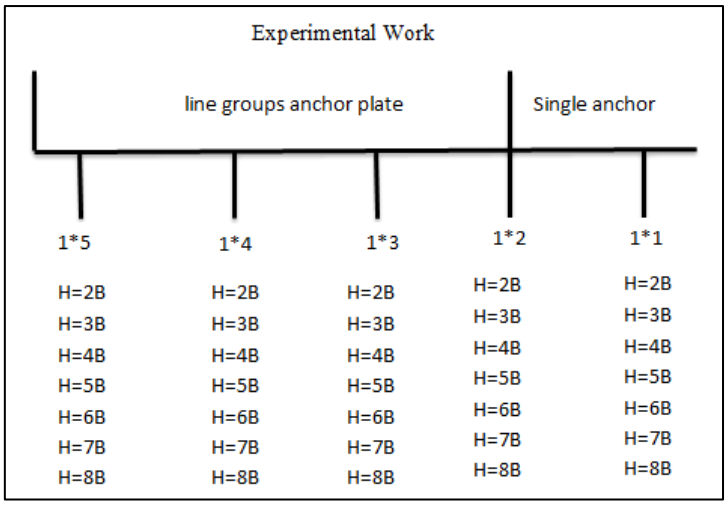


**Figure 2. Overview of Experimental Setup: Line Group Anchor Plates vs. Single Anchors**

## 3. Analysis and Effect of loading for Single Square Anchor Plate

After applying the uplift load to a single anchor plate, loading continued until the anchor reached the failure mode, which was identified when the load cell reading decreased after reaching its maximum value. The results were then plotted by relating the embedment depth to the vertical displacement and ultimate uplift capacity, as shown in Figures 3 and 4.

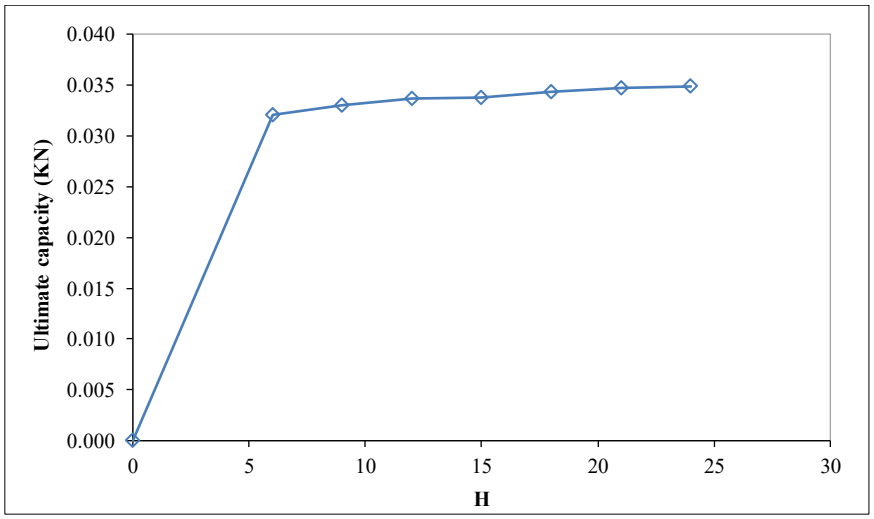


**Figure 3. Relation between the embedded depth and ultimate uplift capacity**

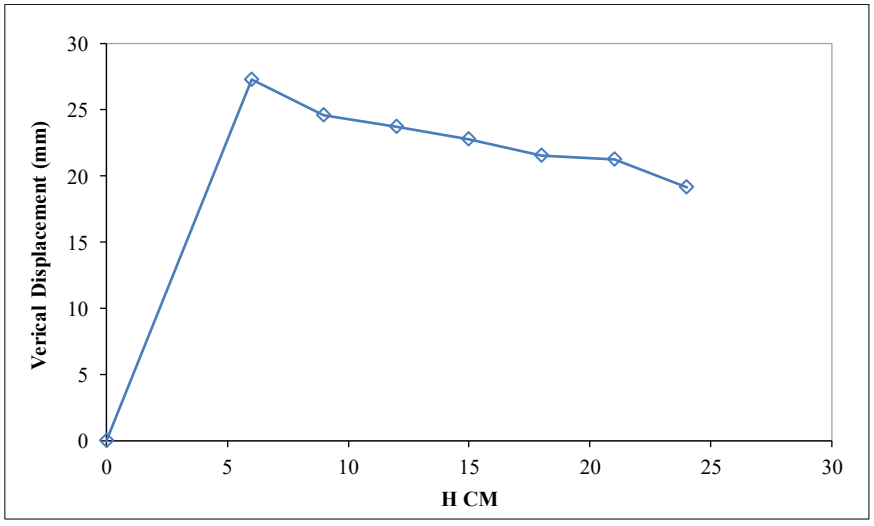


**Figure 4. Relation between the embedded depth and vertical displacement**

According to Figure 3, variations in the embedment depth (H) of the anchor plate lead to an increase in the ultimate uplift capacity of the anchor. This indicates that the soil mass above the anchor plate contributes to carrying the applied load, which increases the load required to bring the system to failure. In other words, the increased overburden weight acting on the plate results in a higher ultimate uplift capacity. In contrast, as shown in Figure 4, increasing the embedment depth (H) leads to a decrease in vertical displacement. This explains why deeper embedment depths exhibit smaller displacement values than shallower depths, due to the increase in the overlying soil mass. As the drag force continues to increase, the soil mass directly above the slab can no longer resist the force independently. Consequently, the slab begins to pull a larger surrounding soil mass upward. This soil mass that moves together with the slab is referred to as the drag zone or resistance zone.

Mathematically, the analysis of the results using the SPSS program to determine the best relationship between embedment depth (H) and ultimate uplift capacity showed that the cubic model has the highest coefficient of determination ($R^2$). This model explains 98.7% of the variation in uplift capacity, making it a highly accurate predictive tool based on embedment depth, as presented in Table 1. If the P-value (Sig.) is less than 0.05, the relationship between the number of anchors and vertical displacement is considered statistically significant, indicating that the effect is real and not due to chance. Conversely, if the P-value is greater than 0.05, the relationship is not statistically significant. In this study, all P-values were less than 0.05. The final equation is presented in Equation 1.

$$Q\ Ult. = 0.001(H) - 3.189 * 10^{-5}(H^2) + 5.728 * 10^{-7}(H^3) + 0.029 \quad (1)$$

where, $Q\ Ult.$: ultimate uplift capacity (KN), $H$: Embedded depth (cm).

**Table 1. Model Summary and Parameter Estimates**

| Dependent Variable: Ultimate Load | | | | | | | | | |
|---|---|---|---|---|---|---|---|---|---|
| Equation | Model Summary | | | | | Parameter Estimates | | | |
| | R Square | F | df1 | df2 | Sig. | Constant | b1 | b2 | b3 |
| Linear | 0.934 | 70.458 | 1 | 5 | 0.000 | 0.032 | 0.000 | | |
| Logarithmic | 0.986 | 348.569 | 1 | 5 | 0.000 | 0.029 | 0.002 | | |
| Inverse | 0.967 | 145.269 | 1 | 5 | 0.000 | 0.036 | -0.022 | | |
| Quadratic | 0.978 | 90.373 | 2 | 4 | 0.000 | 0.030 | 0.000 | -6.117E-6 | |
| Cubic | 0.987 | 78.365 | 3 | 3 | 0.002 | 0.029 | 0.001 | -3.189E-5 | 5.728E-7 |
| Compound | 0.928 | 64.223 | 1 | 5 | 0.000 | 0.032 | 1.004 | | |
| Power | 0.985 | 321.226 | 1 | 5 | 0.000 | 0.029 | 0.059 | | |
| S | 0.971 | 165.336 | 1 | 5 | 0.000 | -3.335 | -0.649 | | |
| Growth | 0.928 | 64.223 | 1 | 5 | 0.000 | -3.453 | 0.004 | | |
| Exponential | 0.928 | 64.223 | 1 | 5 | 0.000 | 0.032 | 0.004 | | |
| Logistic | 0.928 | 64.223 | 1 | 5 | 0.000 | 31.607 | 0.996 | | |

The independent variable is Embedded Depth.

And the graphs of estimated models are shown in Figure 5. The primary purpose of this graph is to visually compare the eleven models to determine which best fits the observed data. The best model, the cubic curve, is most likely the line that passes closest to most of the observed points (the actual data), because it has the highest $R^2$ value (0.987) in the accompanying table. This means that its curved shape (which may be a gentle S-shape or a curve with three inflection points) accurately describes the nonlinear relationship between depth and extraction capacity.

While the best relationship between embedded depth (H) and vertical displacement showed the cubic has the highest R-squared, as shown in Table 2, The highest $R^2$ value is 0.988 (or 98.8%) for the cubic model. This means that the cubic model explains 98.8% of the variation in the data, making it the best model among all tested models. F (F-statistic): Tests the statistical significance of the model as a whole. The values are generally high, and the significance level (Sig.) is 0.000 or 0.001 for all models, confirming that they are all strongly statistically significant (better than a model with

no independent variable). df1 and df2 (degrees of freedom) are related to the F-statistic. Sig. (statistical significance - p-value), and all values are less than 0.05, indicating that all models are statistically significant. And the graphs of estimated models are shown in Figure 6. The best model, the cubic curve, is most likely the line that passes closest to most of the observed points (the actual data), because it has the highest $R^2$ value (0.987) in the accompanying table. The final equation is as written in Equation 2.

$$Vertical\ Dis. = -2.237(H) + 0.127(H^2) - 0.003(H^3) + 36.645 \quad (2)$$

where, $Vertical\ Dis.$: vertical displacement (mm) and $H$: Embedded depth (cm).

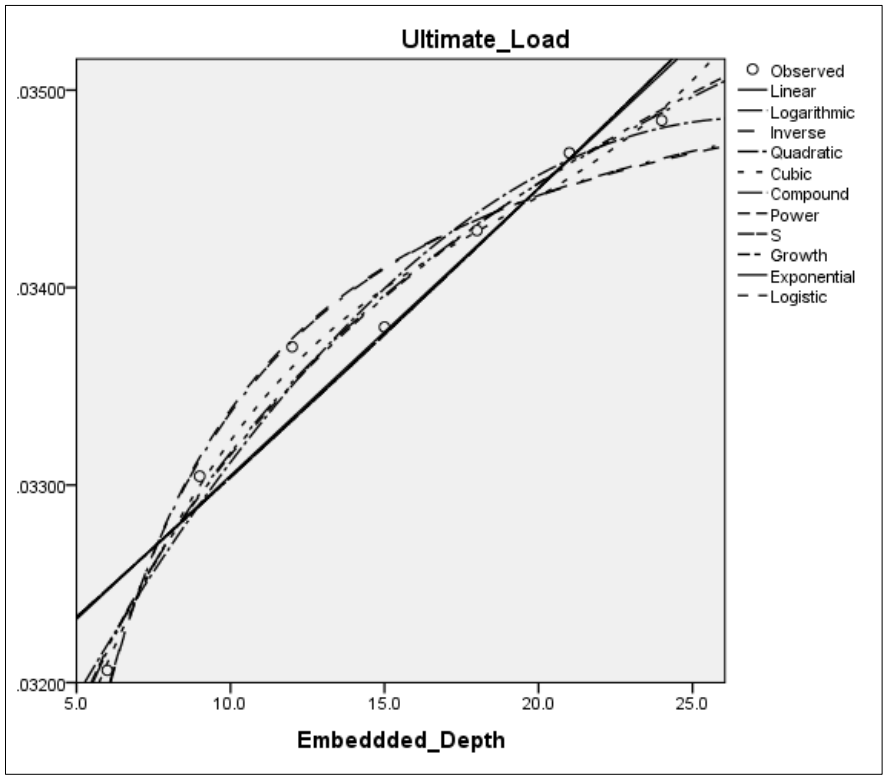


**Figure 5. Model Summary and Parameter Estimates**

**Table 2. Model Summary and Parameter Estimates**

| Dependent Variable: Vertical Dis. | | | | | | | | | |
|---|---|---|---|---|---|---|---|---|---|
| Equation | Model Summary | | | | | Parameter Estimates | | | |
| | R Square | F | df1 | df2 | Sig. | Constant | b1 | b2 | b3 |
| Linear | 0.954 | 103.434 | 1 | 5 | 0.000 | 28.824 | -0.395 | | |
| Logarithmic | 0.967 | 144.316 | 1 | 5 | 0.000 | 36.575 | -5.233 | | |
| Inverse | 0.916 | 54.770 | 1 | 5 | 0.001 | 18.261 | 56.681 | | |
| Quadratic | 0.963 | 51.395 | 2 | 4 | 0.001 | 30.192 | -0.612 | 0.007 | |
| Cubic | 0.989 | 93.986 | 3 | 3 | 0.002 | 36.645 | -2.237 | 0.127 | -0.003 |
| Compound | 0.962 | 125.496 | 1 | 5 | 0.000 | 29.482 | 0.983 | | |
| Power | 0.952 | 99.292 | 1 | 5 | 0.000 | 41.051 | -0.225 | | |
| S | 0.882 | 37.375 | 1 | 5 | 0.002 | 2.928 | 2.414 | | |
| Growth | 0.962 | 125.496 | 1 | 5 | 0.000 | 3.384 | -0.017 | | |
| Exponential | 0.962 | 125.496 | 1 | 5 | 0.000 | 29.482 | -0.017 | | |
| Logistic | 0.962 | 125.496 | 1 | 5 | 0.000 | 0.034 | 1.017 | | |

The independent variable is Embedded Depth.

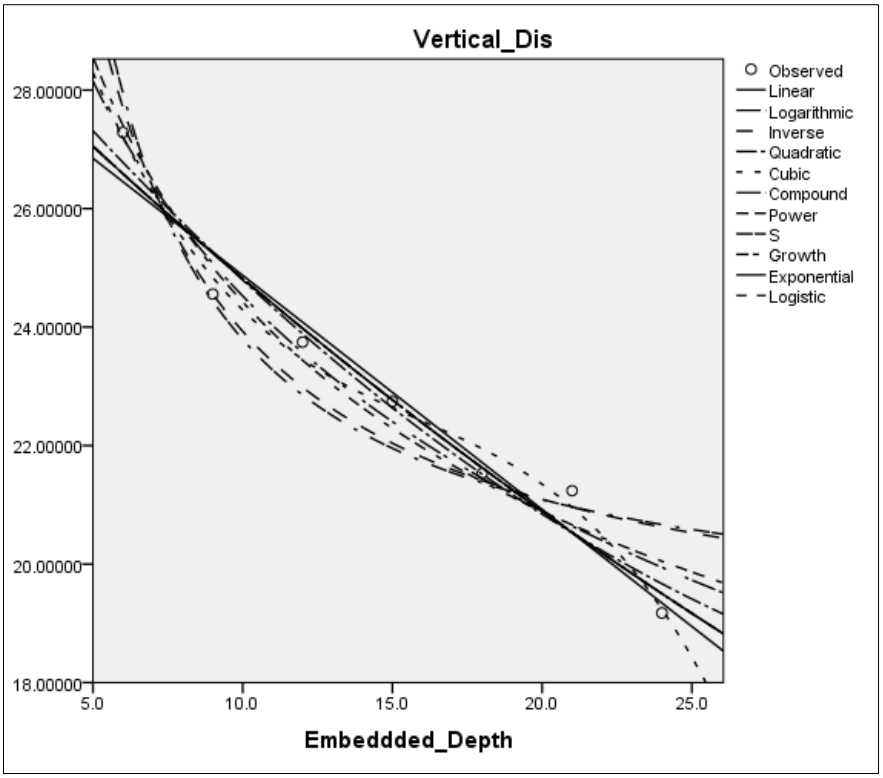


**Figure 6. Model Summary and Parameter Estimates**

## 4. Analysis and Effect of Loading for Line Group Square Anchor Plate

After applying the uplift load to the square anchor plate line groups until the anchors reached the failure mode—at which point the load cell reading decreased after reaching its maximum value—the results were plotted in terms of embedment depth versus vertical displacement and ultimate uplift capacity for the line groups (1×2), (1×3), (1×4), and (1×5), as shown in Figures 7 and 8. As indicated in Figure 6, the increase in ultimate uplift capacity is proportional to the increase in the number of anchor plates. This demonstrates that the applied load is distributed among the anchor plates, and the group behaves as a single large anchor plate when the spacing is S = 4D (B) [24].

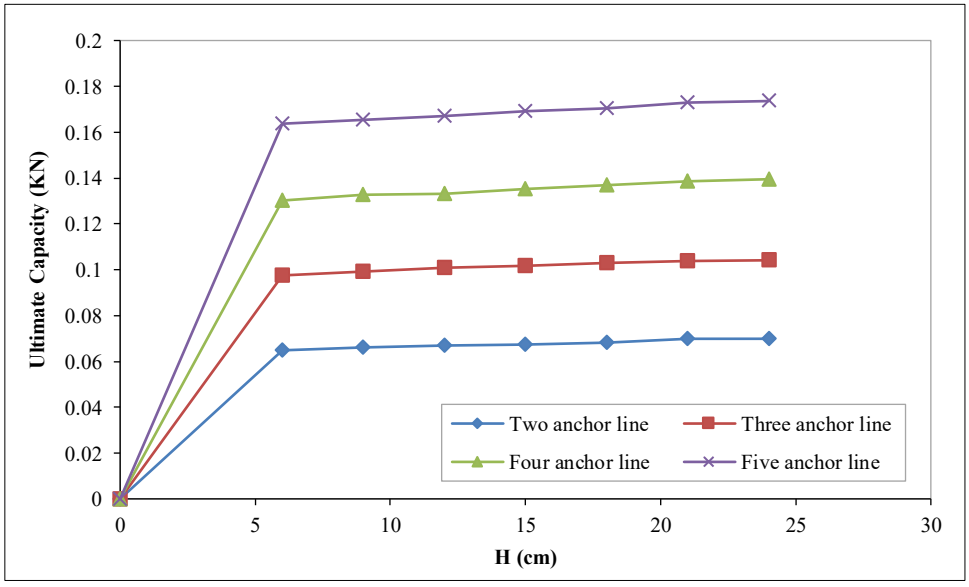


**Figure 7. Relation between the embedded depth and ultimate uplift capacity**

As shown in Figure 8, for anchor groups consisting of two and three anchors, increasing the number of anchors from two to three results in a decrease in vertical displacement at failure, as the system tends to stabilize the surrounding soil. When the embedment depth of the anchor plate increases, the soil's resistance to pullout also increases due to the rise in internal friction along the anchor shaft, leading to a reduction in vertical displacement during uplift loading. However,

when the number of anchors exceeds four in line groups, the vertical displacement increases instead of decreasing. This indicates that having more than four anchors leads to dissociation and a reduction in the physical strength between soil particles.

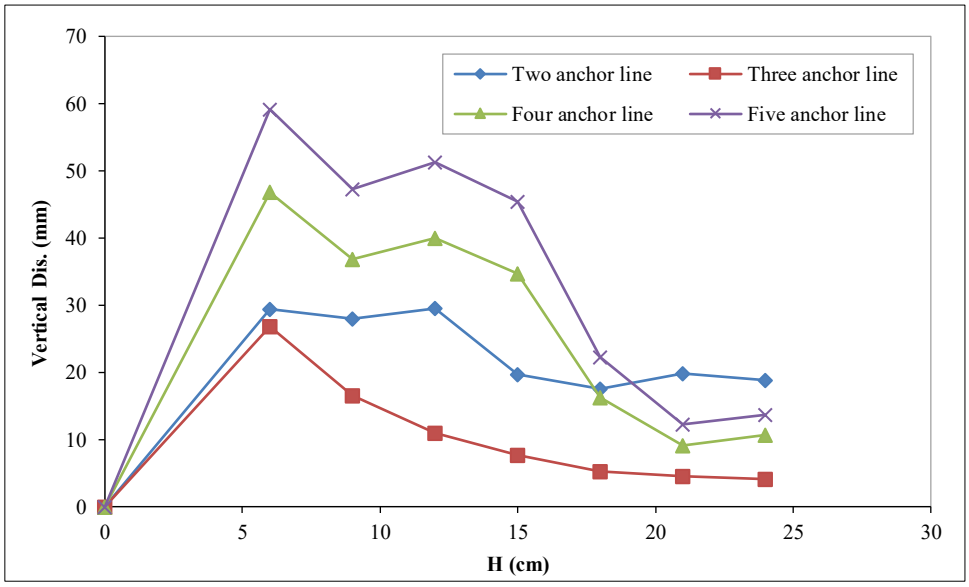


**Figure 8. Relation between the embedded depth and vertical displacement**

For anchor groups, the reduction in vertical displacement occurs because the applied force lifts a larger soil mass with greater inertia. As a result, the rate of vertical displacement decreases significantly with each increase in drag force. In other words, a substantial increase in force is required to lift this heavy mass by a very small distance. At a certain point, the force may increase dramatically while the displacement remains nearly zero, indicating that the drag zone has fully formed and reached its maximum load-bearing capacity. Statistically, the best relationship between embedment depth and ultimate uplift capacity is presented in Table 3.

**Table 3. Model Summary [a, b]**

| Model | R | R Square | Adjusted R Square | Std. Error of the Estimate | Durbin-Watson |
|---|---|---|---|---|---|
| 1 | 1.000 [a] | 1.000 | 1.000 | 0.00026854 | 2.245 |

a. Predictors: (Constant), No_of_anchors, embedded depth.

b. Dependent Variable: Ultimate Capacity

The correlation coefficient for the mathematical models is R = 1, which indicates the presence of a very strong correlation between the independent variables (embedment depth and number of anchors). The coefficient of determination reflects the quality of the regression model and the strength of the influence. It is represented by the square of the correlation coefficient ($R^2$), which has a value of 1, indicating a strong influence. In other words, the independent variables (embedment depth and number of anchors) explain 100% of the variation in the dependent variable (ultimate uplift capacity).

In contrast, Table 4 refers to the relationship between the independent variables (embedment depth and number of anchors) and the dependent variable (vertical displacement). It is evident that vertical displacement depends on factors other than embedment depth and number of anchors, as the coefficient of determination has a value of $R^2 = 0.437$. This means that 56.3% of the variation in vertical displacement is influenced by other factors, such as loading duration (creep effects), soil unit weight, plate shape and dimensions, internal friction, and moisture content. However, these factors have a relatively low influence on the ultimate uplift capacity, as indicated in Table 3.

**Table 4. Model Summary [a, b]**

| Model | R | R Square | Adjusted R Square | Std. Error of the Estimate | Durbin-Watson |
|---|---|---|---|---|---|
| 1 | 0.661[a] | 0.437 | 0.156 | 7.510 | 2.622 |

a. Predictors: (Constant), No_of_anchors. embedded depth

b. Dependent Variable: Vertical_Dis.

## 5. Statistical Analysis for Single and Line Group Square Anchor Plate

Based on the statistical models developed for single and line group square anchor plates, a strong relationship was observed between the number of anchors and the ultimate uplift capacity using linear, quadratic, cubic, and power models, as presented in Table 5. This indicates that the ultimate capacity depends significantly on the number of anchors, with a strong correlation expressed by the linear relationship shown in Equation 3.

$$Q\ Ult. = 0.035(No.A) - 0.004 \quad (3)$$

where, $Q\ Ult.$: ultimate uplift capacity (KN) and $No.A$: number of anchors.

**Table 5. Model Summary and Parameter Estimates**

| Dependent Variable: Ultimate_Capacity | | | | | | | | | |
|---|---|---|---|---|---|---|---|---|---|
| Equation | Model Summary | | | | | Parameter Estimates | | | |
| | R Square | F | df1 | df2 | Sig. | Constant | b1 | b2 | b3 |
| Linear | 1.000 | 92359.186 | 1 | 3 | 0.000 | -0.004 | 0.035 | | |
| Logarithmic | .946 | 52.824 | 1 | 3 | 0.005 | 0.021 | 0.086 | | |
| Inverse | .811 | 12.865 | 1 | 3 | 0.037 | 0.174 | -0.156 | | |
| Quadratic | 1.000 | 31692.749 | 2 | 2 | 0.000 | -0.003 | 0.035 | 2.890E-5 | |
| Cubic | 1.000 | 161487.022 | 3 | 1 | 0.002 | -0.001 | 0.032 | 0.001 | 0.000 |
| Compound | 0.944 | 50.722 | 1 | 3 | 0.006 | 0.026 | 1.508 | | |
| Power | 1.000 | 50376.927 | 1 | 3 | 0.000 | 0.032 | 1.052 | | |
| S | 0.956 | 64.719 | 1 | 3 | 0.004 | -1.510 | -2.014 | | |
| Growth | 0.944 | 50.722 | 1 | 3 | 0.006 | -3.662 | 0.411 | | |
| Exponential | 0.944 | 50.722 | 1 | 3 | 0.006 | 0.026 | 0.411 | | |
| Logistic | 0.944 | 50.722 | 1 | 3 | 0.006 | 38.943 | 0.663 | | |

The independent variable is No_of_anchors.

As illustrated in Figure 9, the cubic, quadratic, and linear models all achieved an $R^2$ value of 1.000. However, the linear model, while simpler, may not adequately capture the curvature present in the data. In contrast, the quadratic and cubic models offer greater flexibility and are capable of representing nonlinear and more complex relationships, making them stronger candidates for describing the best fit to the observed data.

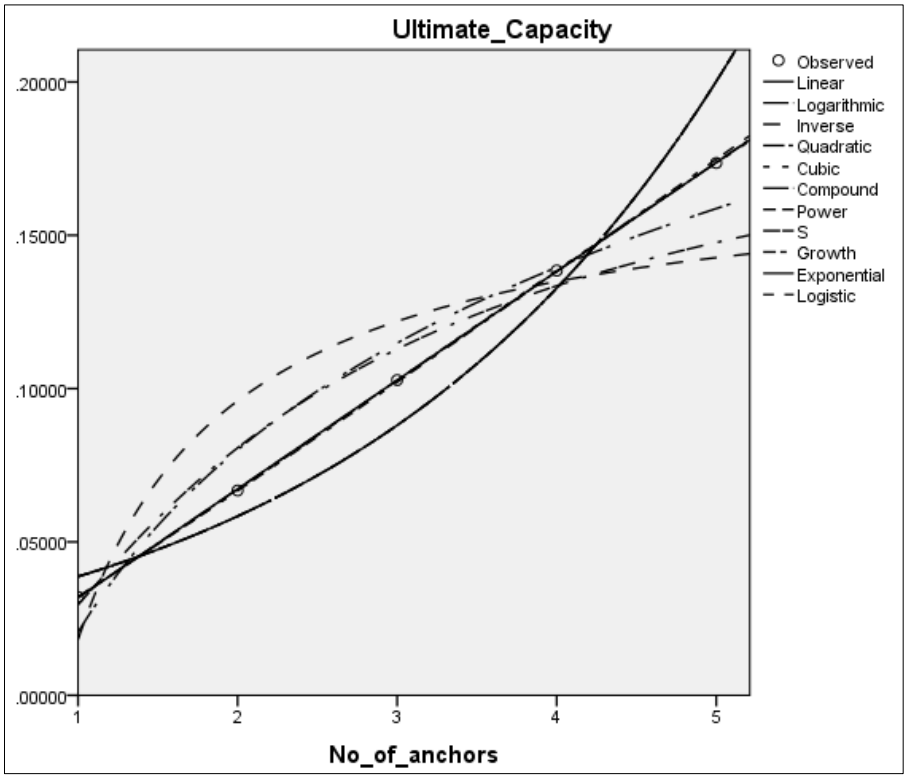


**Figure 9. Model Summary and Parameter Estimates**

In Figure 9 above, various mathematical models are plotted to examine the relationships and to identify the model that best explains the experimental results. The selected model is the one that most accurately represents the test data by passing through the measured points. In contrast, the relationship between vertical displacement and the number of anchors, as shown in Table 6, indicates that the maximum correlation coefficient (R = 0.797) is achieved using the cubic model, as expressed in Equation 4.

$$Vertical\ Dis. = 34.47(No.A) - 17.959(No.A^2) + 2.254(No.A^3) + 9.69 \quad (9)$$

where: $Vertical\ Dis.$: Vertical displacement (mm) and $No.A$: number of anchors.

**Table 6. Model Summary and Parameter Estimates**

| Dependent Variable: Vertical_Dis | | | | | | | | | |
|---|---|---|---|---|---|---|---|---|---|
| Equation | Model Summary | | | | | Parameter Estimates | | | |
| | R Square | F | df1 | df2 | Sig. | Constant | b1 | b2 | b3 |
| Linear | 0.482 | 2.789 | 1 | 3 | 0.193 | 31.276 | -4.768 | | |
| Logarithmic | 0.545 | 3.586 | 1 | 3 | 0.155 | 29.047 | -12.610 | | |
| Inverse | 0.510 | 3.121 | 1 | 3 | 0.175 | 6.055 | 23.907 | | |
| Quadratic | 0.642 | 1.796 | 2 | 2 | 0.358 | 47.555 | -18.721 | 2.326 | |
| Cubic | 0.797 | 1.312 | 3 | 1 | 0.553 | 9.690 | 34.470 | -17.959 | 2.254 |
| Compound | 0.309 | 1.340 | 1 | 3 | 0.331 | 30.118 | 0.774 | | |
| Power | 0.401 | 2.011 | 1 | 3 | 0.251 | 28.005 | -0.726 | | |
| S | 0.416 | 2.134 | 1 | 3 | 0.240 | 1.976 | 1.448 | | |
| Growth | 0.309 | 1.340 | 1 | 3 | 0.331 | 3.405 | -0.256 | | |
| Exponential | 0.309 | 1.340 | 1 | 3 | 0.331 | 30.118 | -0.256 | | |
| Logistic | 0.309 | 1.340 | 1 | 3 | 0.331 | 0.033 | 1.292 | | |

The independent variable is No_of_anchors.

Figure 10 presents the relationship curves, illustrating the strongest statistical relationships that approximately pass through the actual data points and thus provide reliable predictions of the expected values.

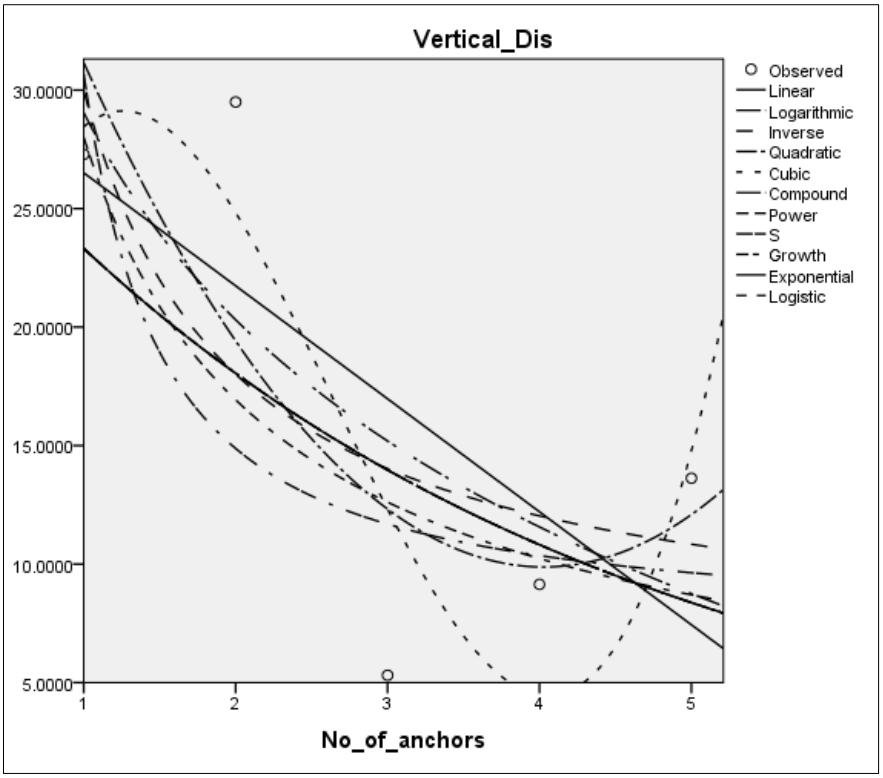


**Figure 10. Model Summary and Parameter Estimates**

## 6. Conclusion

There is a strong correlation between the ultimate uplift capacity and both the embedded depth and the number of anchor plates. However, there is insufficient correlation between vertical displacement and the embedded depth and number of anchor plates. When the number of anchor plates increases to three, the vertical displacement decreases. The influence of embedded depth and number of anchor plates alone is not mathematically sufficient to explain vertical displacement, indicating that other factors affect this response. The bonding forces between sandy soil particles become physically weaker as the number of anchor plates increases. Nevertheless, statistical analysis confirms a strong correlation between the maximum uplift force of anchors installed in sandy soil and both the embedded depth and the number of anchors.

The reduction in vertical displacement with increasing drag force indicates a transition in anchor behavior from the sticking phase to the mass-lifting (displacement) phase, which represents the intended and desirable behavior, as it provides higher load-bearing capacity. As the embedded depth increases, the ultimate bearing capacity also increases, while the vertical displacement decreases as the anchor is pulled upward. Additionally, increasing the number of anchors is directly proportional to the changes associated with increased embedded depth, except in cases where the number of anchors exceeds three.

## 7. Declarations

### 7.1. Author Contributions

Conceptualization, A.R.D. and A.A.A.; methodology, A.A.A. and A.R.D.; software, A.R.D.; validation, A.A.A.; formal analysis, A.R.D.; investigation, A.R.D.; resources, A.R.D. and A.A.A.; data curation, A.R.D.; writing—original draft preparation, A.R.D.; writing—review and editing, A.R.D. and A.A.A.; visualization, A.A.A.; supervision, A.A.A.; project administration, A.A.A.; funding acquisition, A.R.D. All authors have read and agreed to the published version of the manuscript.

### 7.2. Data Availability Statement

The data presented in this study are available on request from the corresponding author.

### 7.3. Funding

The authors received no financial support for the research, authorship, and/or publication of this article.

### 7.4. Conflicts of Interest

The authors declare no conflict of interest.

## 8. References

[1] O'neill, M. P., O'loughlin, C. D., Watson, P. G., Gaudin, C., Palacios, M., Stubbs, J., & Kuo, M. (2023). Broadening the use of SEPLAs for floating wind applications - anchoring in non-clay soils. 9th International SUT Offshore Site Investigation Geotechnics Conference Proceedings "Innovative Geotechnologies for Energy Transition," 1249–1255. doi:10.3723/SOIC4915.

[2] Cerfontaine, B., White, D., Kwa, K., Gourvenec, S., Knappett, J., & Brown, M. (2023). Anchor geotechnics for floating offshore wind: Current technologies and future innovations. Ocean Engineering, 279, 114327. doi:10.1016/j.oceaneng.2023.114327.

[3] Chow, S. H., Diambra, A., O'Loughlin, C. D., Gaudin, C., & Randolph, M. F. (2020). Consolidation effects on monotonic and cyclic capacity of plate anchors in sand. Geotechnique, 70(8), 720–731. doi:10.1680/jgeot.19.TI.017.

[4] Roy, A., Chow, S. H., Randolph, M. F., & O'loughlin, C. D. (2022). Consolidation effects on uplift capacity of shallow horizontal plate anchors in dilating sand. Geotechnique, 72(11), 957–973. doi:10.1680/jgeot.20.P.117.

[5] Cao, J., Audibert, J. M. E., Al-Khafaji, Z., Phillips, R., & Popescu, R. (2002, May). Numerical analysis of the behavior of suction caissons in clay. ISOPE International Ocean and Polar Engineering Conference (pp. ISOPE-I), 26-31 May, 2002, Kitakyushu, Japan.

[6] Mana, D. S. K., Gourvenec, S., & Randolph, M. F. (2014). Numerical modelling of seepage beneath skirted foundations subjected to vertical uplift. Computers and Geotechnics, 55, 150–157. doi:10.1016/j.compgeo.2013.08.007.

[7] Maitra, S., White, D., Chatterjee, S., & Choudhury, D. (2019). Numerical modelling of seepage and tension beneath plate anchors. Computers and Geotechnics, 108, 131–142. doi:10.1016/j.compgeo.2018.12.022.

[8] Maitra, S., Chatterjee, S., White, D., & Choudhury, D. (2022). Uplift resistance of buried pipelines: The contribution of seepage forces. Ocean Engineering, 250, 111037. doi:10.1016/j.oceaneng.2022.111037.

[9] Mors, H. (1959). The behaviour of mast foundations subjected to tensile forces. Bautechnik, 36(10), 367-378.

[10] Fujiwara, Y., Murakami, T., Fukuda, M., Takashima, M., & Nagaki, H. (2019). A Study on Tensile Force Management Method for Additional Ground Anchor Construction Implemented as a Deterioration Countermeasure. Journal of Japan Society of Civil Engineers, Ser. C (Geosphere Engineering), 75(1), 115-130. doi:10.2208/JOURNALOFJSCE.8.1_161.

[11] Park, B., Kim, W., Hwang, S., & Kwon, O. (2020). A study on the cut-slope maintenance according to anchor tension force. Journal of Engineering Geology, 30(4), 673–682. doi:10.9720/kseg.2020.4.673. (In Korean).

[12] Park, S. Y., Lee, S., Jung, J., & Cho, W. (2020). Evaluation of residual tensile load of field ground anchors based on long-term measurement. Journal of the Korean Geotechnical Society, 36(8), 35-47. doi:10.7843/kgs.2020.36.

[13] Sic Choi, T., Mann Yun, J., Seong Kim, Y., Kyong You, S., & Il Lee, K. (2021). Stability Evaluation of Anchors Using Lift-off Field Test. Journal of the Society of Disaster Information, 17(1), 128–142. doi:10.15683/kosdi.2021.3.31.128.

[14] Ovesen, N. K., & Strømann, H. (1972). Design method for vertical anchor slabs in sand. Performance of earth and earth-supported structures, American Society of Civil Engineers (ASCE), Reston, United States.

[15] Meyerhof, G. G. (1975). Uplift resistance of inclined anchors and piles. International Journal of Rock Mechanics and Mining Sciences & Geomechanics Abstracts, 12(7), 97. doi:10.1016/0148-9062(75)90476-3.

[16] Kame, G. S., Dewaikar, D. M., & Choudhury, D. (2012). Pullout Capacity of a Vertical Plate Anchor Embedded in Cohesion-less Soil. Earth Science Research, 1(1), 27–56. doi:10.5539/esr.v1n1p27.

[17] Jadid, R., Abedin, M. Z., Rafat Shahriar, A., & Uddin Arif, M. Z. (2018). Analytical Model for Pullout Capacity of a Vertical Concrete Anchor Block Embedded at Shallow Depth in Cohesionless Soil. International Journal of Geomechanics, 18(7), 6018017. doi:10.1061/(asce)gm.1943-5622.0001212.

[18] Shahriar, A. R., Islam, M. S., & Jadid, R. (2020). Ultimate Pullout Capacity of Vertical Anchors in Frictional Soils. International Journal of Geomechanics, 20(2), 4019153. doi:10.1061/(asce)gm.1943-5622.0001576.

[19] Hao, D., Chen, X., Chen, R., & Yuan, C. (2024). Numerical Investigation on Uplift Capacity and Failure Mode of Inclined Circular Plate/Helical Anchor in Sand. Volume 8: Offshore Geotechnics; Petroleum Technology. doi:10.1115/omae2024-134450.

[20] Hassan, M. M., Rahman, N., Rokonuzzaman, M. D., & Rahman, S. (2024). Effect of anchor geometry on uplift resistance of plate anchor in sloping terrain. Ocean Engineering, 292, 116498. doi:10.1016/j.oceaneng.2023.116498.

[21] Wang, J., Xia, H., Cai, H., & Hua, J. (2024). Study on the influence of anchor plate parameters on the bearing characteristics of the new large-diameter multi-plate soil anchor and creep property of anchor. Scientific Reports, 14(1), 28158. doi:10.1038/s41598-024-79783-4.

[22] Buragadda, V., Orekanti, E. R., Garu, V. Y., & Edagotti, P. K. (2024). Influence of Reinforcement Geometrical Parameters on Plate Anchor Uplift Capacity. Transportation Infrastructure Geotechnology, 11(4), 1828–1859. doi:10.1007/s40515-023-00351-w.

[23] Daibil, A. R., & Al-Saidi, A. A. H. (2025). The Soil-Anchors System Theories and Improvement: A Review Study. Journal of Engineering, 31(7), 167–197. doi:10.31026/j.eng.2025.07.10.

[24] Larnach, W. J., & Mcmullan, D. J. (1975). Paper 19 Behaviour of inclined groups of plate anchors in dry sand. Diaphragm Walls & Anchorages, 153–156, Emerald Publishing, Leeds, United Kingdom. doi:10.1680/dwaa.00056.0024.